A new concept of precast concrete retaining wall: from laboratory model to the in-situ tests

Tan Trung Bui, H. V. Tran, A. Limam, M. Bost, Q. Bui, P. Robit

A new concept of precast concrete retaining wall: from laboratory model to the in-situ tests

A new concept of precast concrete retaining wall: from laboratory model to the in-situ tests

T T Bui[1*], H V Tran[1], A Limam[2], M Bost[3], Q B Bui[4], P Robit[5]

[1]University of Lyon, INSA Lyon, SMS-ID, France
[2]University of Lyon, France
[3]GERS-RRO, IFSTTAR, Bron, France
[4]Sustainable Developments in Civil Engineering Research Group, Faculty of Civil Engineering, Ton Duc Thang University, Ho Chi Minh City, Vietnam
[5]GTS Group NGE Lyon, France

[*]Corresponding author, Email: tan-trung.bui@insa-lyon.fr

Abstract. A new concept for the soil nail walls is here proposed and validated through experimental and numerical approaches. This process, based on the use of precast elements that are easier to install, is cheaper and more aesthetic than the classical methods, but the main advantage is reducing the cement consumption which conducts to divided carbon footprint by three. In order to characterize the structural capacity of this new process, this article present an investigation on two *in-situ* representative walls, one in shotcrete which is the old way of construction, and the other, consisting the precast reinforced concrete slabs, which is the new process. We thus have a demonstrator on a real scale, and perfectly representative, since the constructive modes, as well as the mechanical, thermal, and hydric loadings are the real ones associated with the environment in situ. Substantial instrumentation has been realized over a long period (nearly 2 years), enabling to follow the evolution of the displacements of each wall and the efforts in the anchor nails. To determine the bearing capacity of the constituent element of the precast nail wall, an experimental study coupled with a numerical simulation has been conducted in the laboratory on a single precast slab. This study allows the evaluation of the load associated to crack initiation and the bearing capacity associated to the ultimate state, at the scale of the constituent elements. Finally, in order to evaluate the behaviour of the two concepts of nail walls in the case of extreme solicitation, a dynamic loading induced by an explosion has been conducted on the site.

1. Introduction

Soil nailing is a soil retention technique using grouted tension-resisting steel elements that can be used to retain excavations and stabilize steep cut slopes under static and seismic conditions [1]. The case histories and post-earthquake investigations show that soil nail walls have performed well during strong ground motions in contrast with the generally poor performance of gravity retaining structures [2-3]. Knowing that, for the fabrication of a soil nail wall in shotcrete, the quantity of concrete lost by projection rebound is significant, therefore this constructive approach is expensive and damaging from the environmental point of view analysis. An alternative process to shotcrete nail walls was proposed. This process is based on the use of precast elements that are easier to install, cheaper, good quality in bearing capacity as well as aesthetics are better than the shotcrete. To gauge all the parameters, a real scale test was realized and instrumented. To study this new technique, and to compare it with the conventional technique (shotcrete), two representative walls are made: one corresponds to the

conventional shotcrete nail wall (wall 7.50 m high and 10 m wide) and the other to the precast slabs nail wall of same size (Figure 1).

The first phase of this study is to determine the bearing capacity and the associated failure mode of each precast slab which is the constituent element of the precast nail wall in order to verify its design. Then, an experimental study coupled with numerical simulation has been conducted in the laboratory [4], on a precast slab submitted to representative mechanical solicitation. This study allows validating the load associated to crack initiation, cracking behaviour (opening and propagation), and finally, the ultimate state or bearing capacity as well as the associated failure mode.

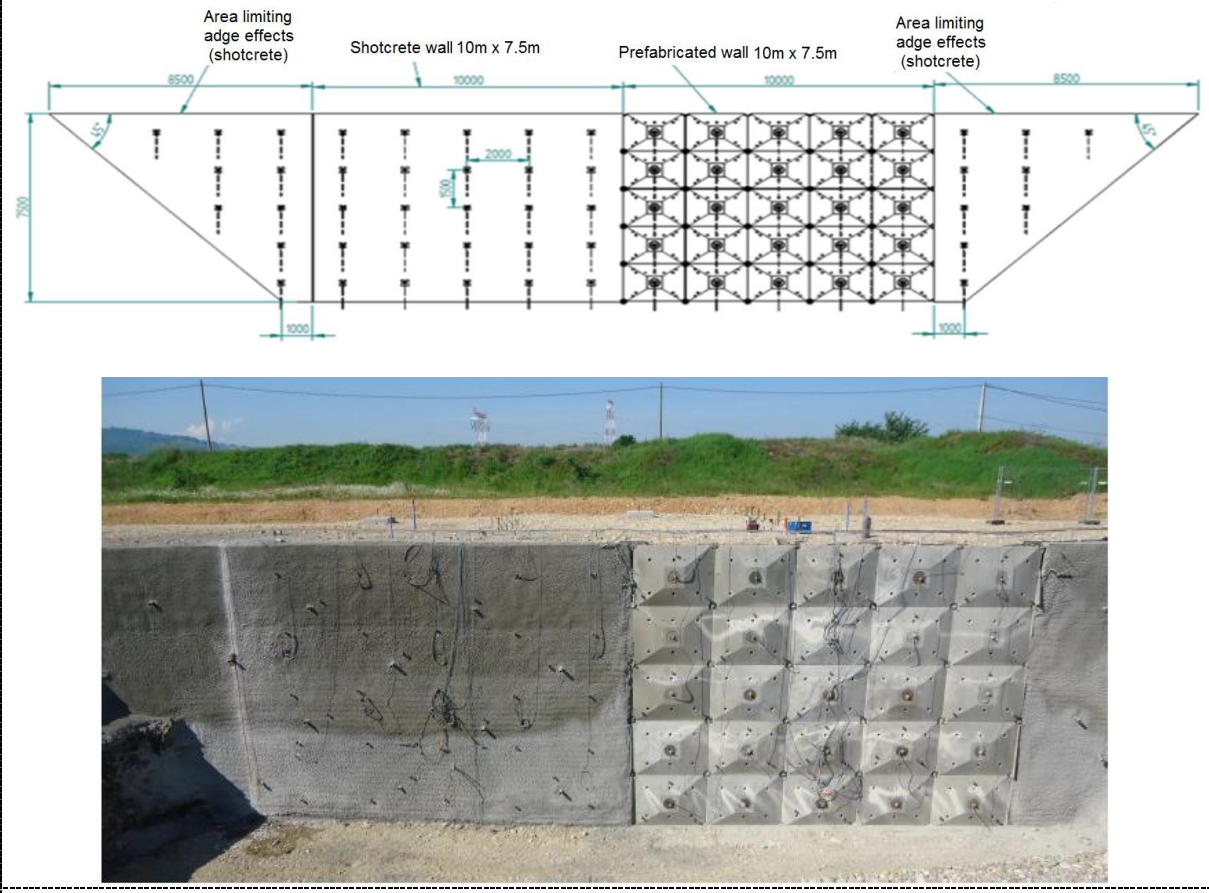

Figure 1. In situ full-scale wall (Rives, Rhône-Alpes, France): shotcrete nail wall - left side; precast nail wall – right side. Unit in [mm]

The second phase is the validation of the behaviour of the full-scale nail wall [5], constructed from the precast slabs which have been tested in the laboratory at the first phase. To assess the efficiency of this new design, a second wall using the shotcrete technique has been constructed next by the precast soil nail wall (Figure 1). The behaviour of the two structures was then analysed thanks to an in situ two years continuous monitoring, where horizontal displacements efforts on the wall and on the anchor nails have been carried out and analysed. Thus, the qualification of the behaviour of the nail wall consisting of precast slabs, compared to the shotcrete wall, could be evaluated, not only on the long term mechanical behaviour, but also on the whole construction phase (economy of material, construction time, ...).

In order to evaluate the behaviour of the two concepts in the case of extreme stress, it is proposed here in the final phase to apply dynamic loading induced by an explosion. Different intensities of the explosion are conducted to evaluate for each level, the behaviour of each configuration, the efforts taken by the nails and the damage of the walls.

2. Laboratory tests

In order to evaluate the behavior of the precast slab under representative mechanical solicitation, two tests are carried out on identical specimens (Figure 2). The objective is to quantify the onset of cracking as well as to evaluate the bearing capacity, and the failure mode. The principle is applying the specimen by a quasi-static force on the central zone on the downstream (top) side. This zone, in fact corresponds to the place where the nail applies on the slab through a hole.

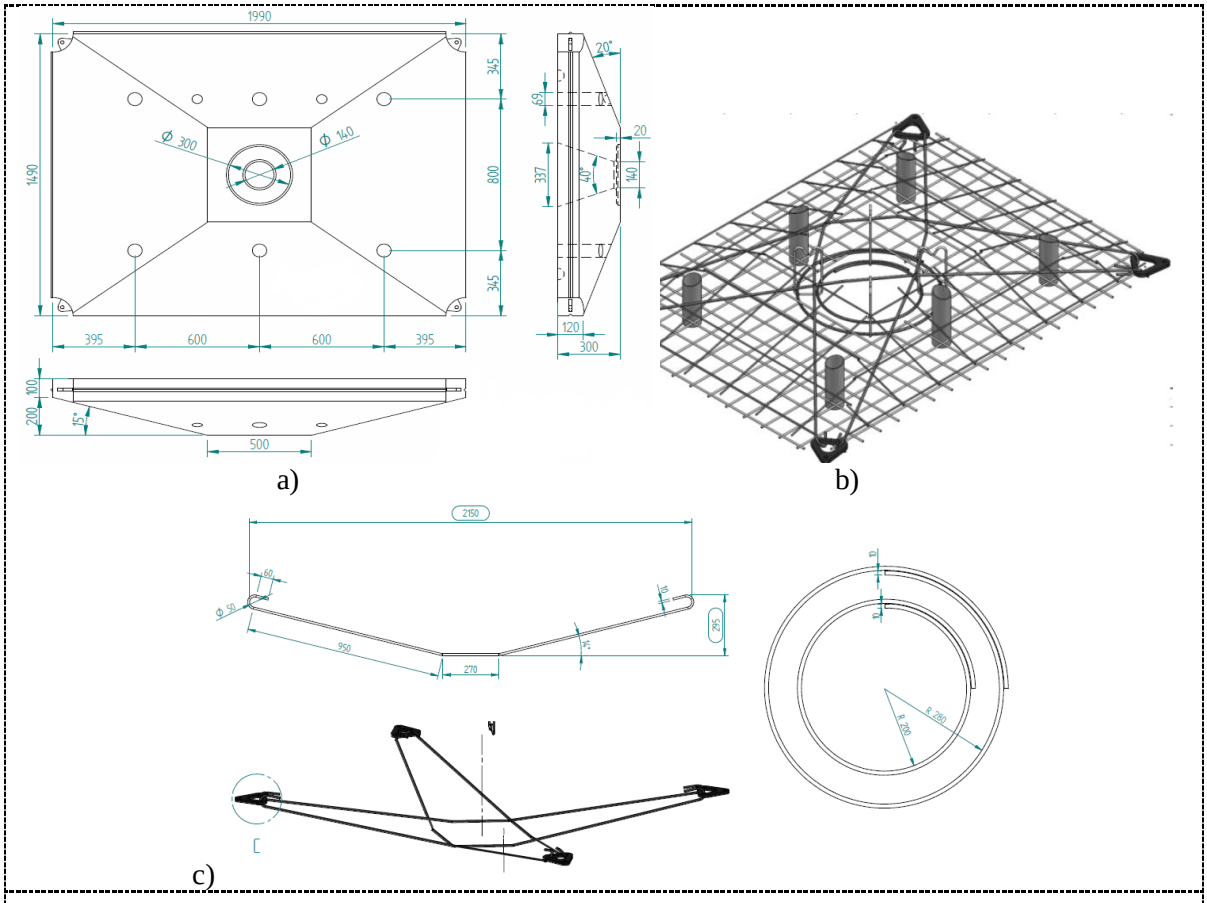

Figure 2. Dimension of the precast concrete slab

2.1. Specimens and test setup

The specimen is supported on four supports (Figure 3). A quasi-static loading was applied (imposed force) on the central zone by a hydraulic jack with a load speed of 1kN/second (60kN/minute). The specimen is instrumented by five displacement sensors LVDT (C1- C5). The specimens were cast using ready-mixed concrete, and a normal strength concrete of class C40/50 was used. The compressive strength of the concrete mixture used for the slabs was determined from compression tests on 11×22-cm cylindrical specimens, performed on the day of slab testing with an average strength of 56.3MPa.

The reinforcement had the yield strength f_y=500 MPa and the ultimate strength f_u=540 MPa. The concrete cover was 30 mm. The amount, the spacing, and the diameter of longitudinal and transverse reinforcement are given in Figure 2. For the lower reinforcement layout, the longitudinal and transversal reinforcement consisted of Ø8 mm placed at an identical distance of 100 mm. For the upper reinforcement layout, the longitudinal and transversal reinforcement consisted of Ø6 mm placed at an identical distance of 200 mm. Two rebar circles placed at the centre of the slab with the diameters of Ø10 mm are used to reinforce the concrete under concentrated load. The cross longitudinal bars used to connecter the slabs through four corners had the diameter of Ø10 mm (Figure 2b).

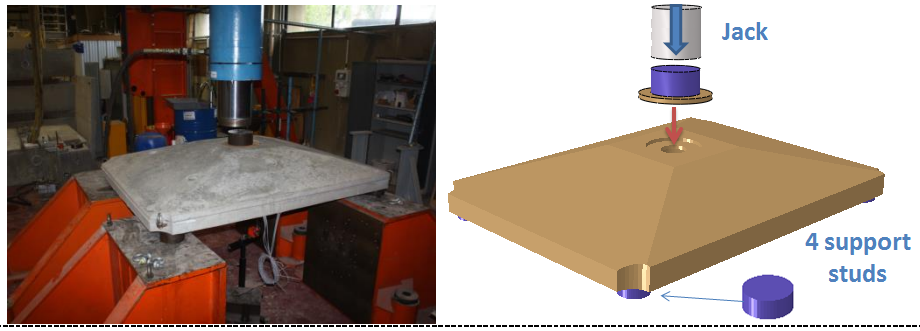

Figure 3. Test setup of the precast concrete slab

2.2. Experimental results

The load/deflection curves of the two tests conducted are shown in Figure 4. The limit of elasticity obtained on the load /deflection curves is about 140kN. The ultimate load is 407kN (specimen 1) and 413kN (specimen 2). Both tests give very similar results, for the bearing capacity the difference is less than 1.5%, and an excellent reproducibility of all the phases characterising the behaviour, from the elastic part at the beginning of loading, to the ultimate state.

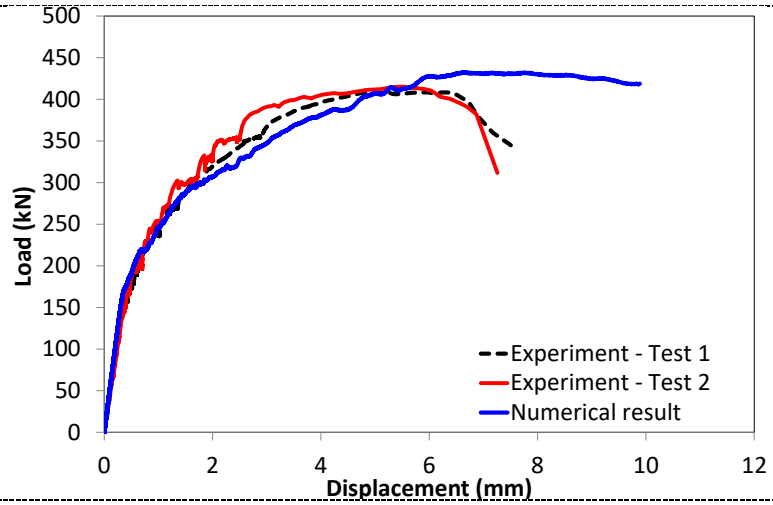

Figure 4. Load/displacement curves: experimental vs numerical results

The failure modes observed for specimen 1 are specified in Figure 5 below. On the bottom face, the rupture due to bending in two ways has been found with the cracks corresponding to the flexural rebar's positions. On the top face, at the four corner of the specimen shear cracks were observed.

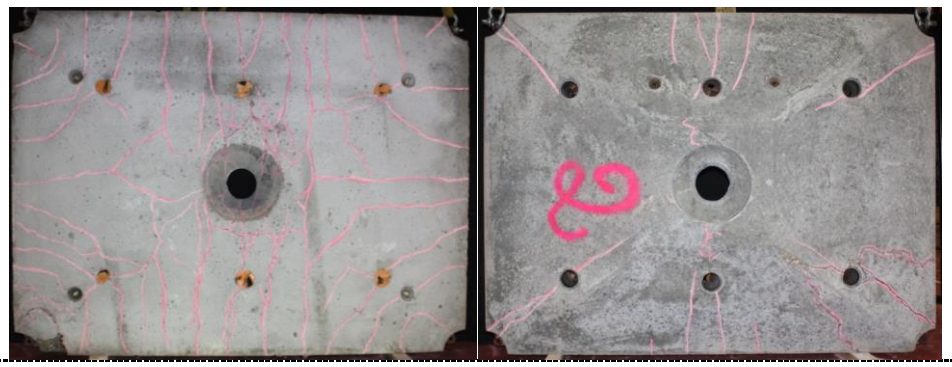

Figure 5. Failure modes of specimen 1: bottom face and top face

2.3. Numerical results

The numerical investigations were conducted with Abaqus software. The failure of RC slabs is sudden, in particular for failure in shear. This could cause numerical instability and convergence problems in the traditional static analysis (implicit analysis). Therefore, the explicit method was used with very small load increments considering a so-called smooth-step function to develop quasi-static analysis. All calculations were made force controlled with an explicit solution technique. In addition, the computing time corresponds to the critical increment size and for FEM with a great number of degrees of freedom; it is considerably shorter in comparison to the computing time under application of implicit solvers. The concrete damaged plasticity model (CDP) in Abaqus was used for concrete material and the elastic-plastic model was applied to reinforcement steel.

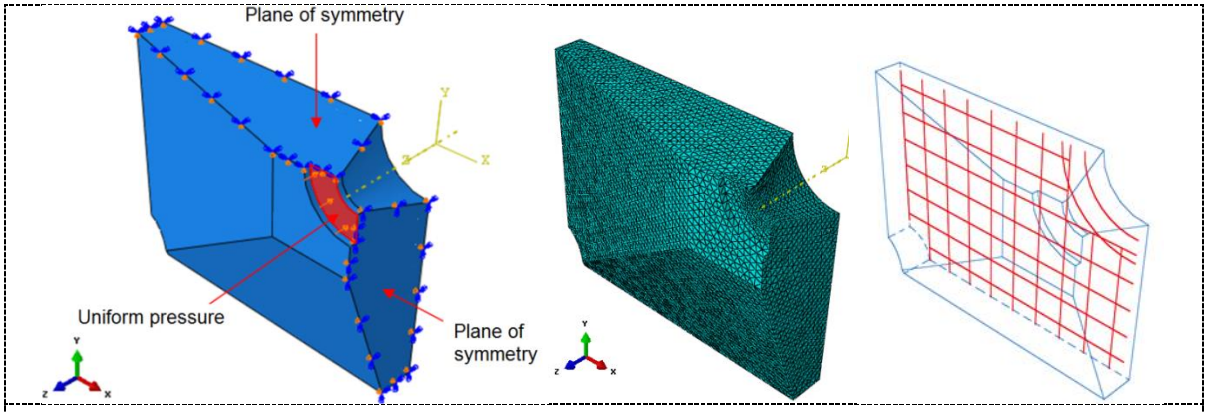

Figure 6. Mesh of the precast slab

The CDP model in Abaqus is based on the models proposed by Lubliner et al. (1989) [3] and (Lee & Fenves, 1998) [7]. The model proposed by Lubliner et al. (1989) [6] for monotonic loading and has been developed later by Lee and Fenves (1998) [7] to consider the dynamic and cyclic loadings. The constitutive theory in this section aims to capture the effects of irreversible damage associated with the failure mechanisms that occur in concrete and other quasi-brittle materials under fairly low confining pressures (less than four or five times the ultimate compressive stress in uniaxial compression loading). The nonlinear behaviour of concrete is attributed to the damage and plasticity processes. The plasticity behaviour can be characterized by several phenomena such as strain softening, progressive deterioration, etc. The damage process can be attributed to micro-cracking. Damage is associated with the concrete's failure mechanisms and therefore results in a reduction in the elastic stiffness. The model based on the concept of isotropic damaged elasticity in combination with isotropic tensile and compressive plasticity to represent the inelastic behaviour of concrete i.e. tensile cracking and compressive crushing.

With the complexity of the selected geometric shape, a 3D finite element model developed on the Abaqus code has been chosen. The modeled geometry is identical to the real geometry and taken into account the presence of the reinforcement (steel) in the concrete slab. Only one quarter of the slab is modeled, taking into account symmetry conditions. The slab rests on 4 supports (Uz blocked unilaterally). Uniform pressure is applied to the central disk of the top surface (Figure 6) in accordance with the experimental test. A perfect adhesion between steel rebars and concrete is assumed. This modeling is fairly faithful to the test.

Table 1. Properties of concrete used in numerical model

Characterictics	Value
Compressive strength f_{cm} (MPa)	56.3
Tensile strength f_{ctm} (MPa)	3.52
Young's modulus (MPa)	35500

Table 2. Properties of steel used in numerical model

Characterictics	Valeurs
Young's modulus (GPa)	210
Yield strength f_{yk} (MPa)	500
Rupture strength (MPa)	540

The characteristics of C40/50 concrete taken from the experimental tests are given in Table 1. For steel reinforcement type Fe500, an elastoplastic model with isotropic hardening is used. The characteristics of the reinforcements are specified in Table 2.

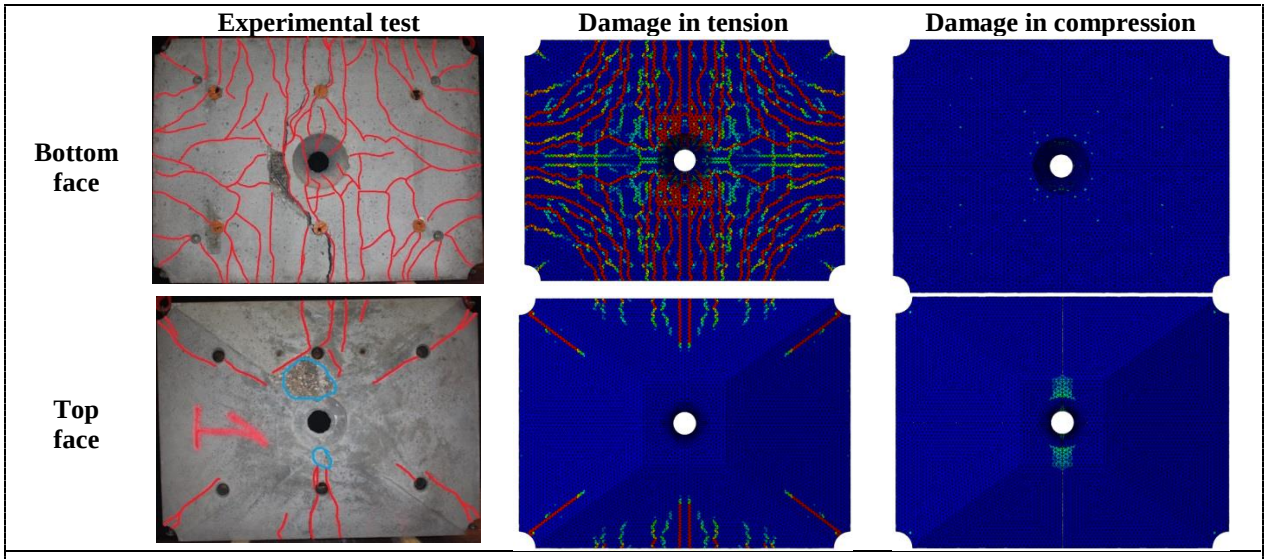

Figure 7. Failure modes: experimental vs numerical results (Specimen 2)

The load/deflection curve obtained numerically at the central point (point instrumented by the sensor C3) is compared with those of the tests (Figure 4). The ultimate load obtained by the numerical computation is of 452 kN, a difference of 11% compared to the experimental result of the test 1 ($P_{exp-test1}$ = 408kN) and of 9% compared to the result of experimental test 2 ($P_{exp-test2}$ = 415kN). The elastic limit (beginning of cracking) is also quite well reproduced by calculation ($P_{elas-FEM}$ = 160kN, $P_{elas-exp}$ = 140kN) a difference of 14% is noticed. The rigidity obtained numerically is similar to that found experimentally, this for the linear phase, but also in the non-linearity phase. The curves in this case are in good adequacy, thus showing the relevance of modeling.

Numerical computation leads to a final failure mode characteristic of bending with essentially two cracks crossing the half-length of the slab. It is confirmed by observing the plastic deformations of longitudinal reinforcement when the ultimate load is reached. The cracking facies are similar between simulation and experiment (Figure7). Using the variables of damage we can visualize the cracking. On the bottom face (tensile face), most cracks are due to traction. On the top face, there is a zone in the center around the hole, where the rupture is obtained by damage in compression of the concrete. This damage is perfectly similar (location) to that observed experimentally (crushing or bursting of the concrete around the hole). Tensile fractures on the top face have developed and prolong the cracks observed initially in the bottom face. They appear at the four corners of the scale, and also on the long span, no crack appears on the smallest span (width) of the scale. This reflects a bending failure but only in one direction, which consolidates a beam-like behavior (one way direction of solicitation). The first cracking observed is the longitudinal crack due to bending. We recall that this test is very conservative in view of the loading that the slab will undergo in situ.

3. Static measurements in situ

On the site located on the city of Rives in the Rhône-Alpes region, France, GTS has built two nail walls. The first comes from a classic construction process, namely a monolithic shotcrete wall which is anchored to the ground with anchor nails. The second concept is an innovation proposed by GTS. The wall here consists of reinforced concrete slabs, each manufactured in prefabrication factory, which are nailed to the ground using an anchor nails.

For the experimental site, five excavations of 1.5m in deep are made all along the wall reaching a theoretical excavated volume of 2200 m3 for a depth of 7.5m. Each excavation phase includes the placement of sealed nails, one nail every two meters horizontally constituting a rectangular mesh with an anchor for each slab for precast elements. This wall consists of five slabs for each row (Figure 8).

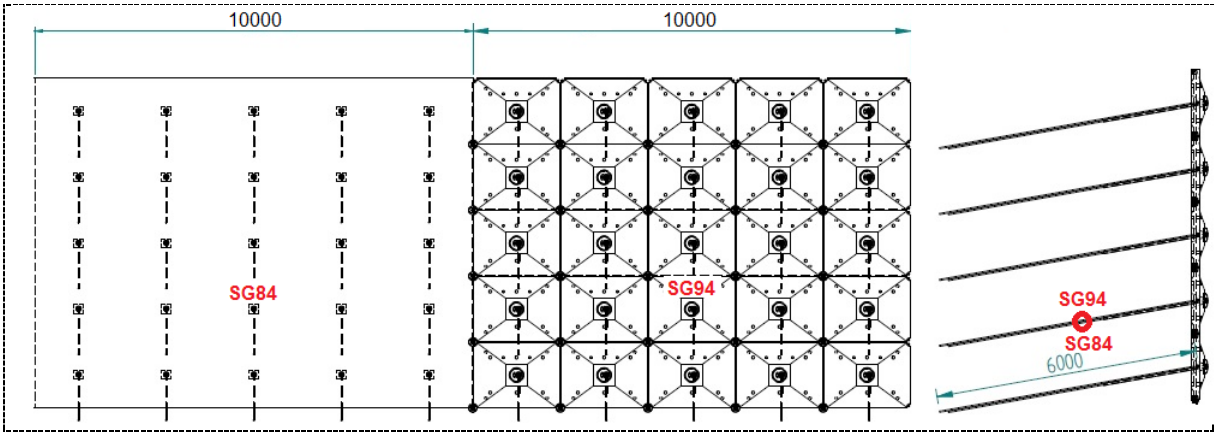

Figure 8. Instrumentation of strain gauges (SG84 and SG94) on the anchor nails

The two walls are instrumented with various sensors, and similarly for the wall of shotcrete and that consisting of precast slabs. The measurement channels quantify either the forces in the nails, using strain gauges, or the pressure on the wall using pressure sensors. We also have a force sensor positioned on a nail. This measure is used to serve as verification. The instrumented points are symmetrically so that the behavior of the shotcrete wall and that of precast slabs can be compared. The study of the quasi-static behavior, which spread over a period of 2 years, is to compare between the two wall behaviors.

Each bar (anchor nail) is equipped with two strain gauges positioned symmetrically on the flats of the bar. This is to take into account any bending of the bar. Figure 9 presents the measures of the two strain gauges in the anchor nail of the shotcrete wall (SG84_01 & SG84_02) and the ones of the precast wall (SG94_01 & SG94_02). The positions of the strain gauges SG84 and SG94 are described in Figure 8. The frequency chosen for our tests is an acquisition every 20 minutes.

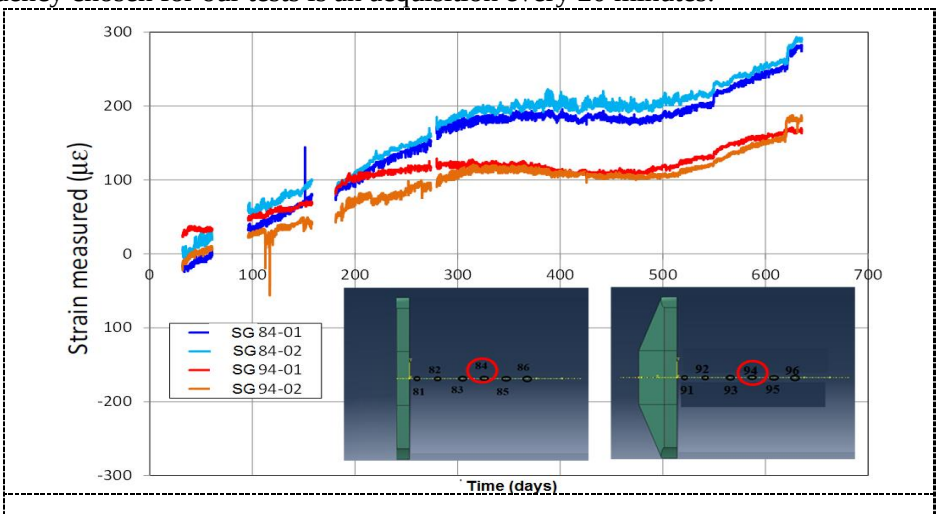

Figure 9. Strain measured on the anchor nails of two walls: SG84 vs SG94

It is noted that the effort is incremented over time, it remains however limited since less than 30 kN (100 με correspond to about 10 kN). It is found that all the sensors give substantially the same orders of magnitude. For this case, perfect equality between the two strain gauges (SG84_01 compared to SG84_02, and SG94_01 compared to SG94_02). We conclude that the nail undergoes a uniform traction. The value of the effort in the precast wall, about 20 kN, is less than the value in the shotcrete wall, about 30 kN (Figure 9). For duration of over 300 days, a plateau equivalent to a load level is reached for two both systems of shotcrete wall and precast wall. Before 500 days we see that the effort varies again and increases (Figure 9).

In this paper, only the measures of two sensors SG84 and SG94 are presented. If the analyses are based on the results of all the sensors, we found that on the majority of the sensors efforts remain low (less than 20 kN with some maximum to 60 kN). Moreover, in many cases there is flexion in the head nail especially for the slabs of precast wall. Apart from a few points where the effort is incremented (from 20 to 40 kN in 2 years), the pushing efforts remain limited. They do not increase in a monotonous way. This is certainly due to a significant "cohesion" of the soil upstream of the nail walls.

4. Explosion tests in situ

In order to evaluate the behavior of the two concepts of nail walls in the case of an extreme load, it is here proposed to apply a dynamic loading induced by an explosion. Three tests are carried out with different intensities of the explosion to evaluate for each level, the behavior of each configuration, the efforts taken by the nails and see the damage of the walls.

Two first tests are conducted with an explosion of a low intensity. For the first shot the amount of explosive that remains low is positioned away from the wall, while for the second shot, the same amount of explosive is positioned close to the wall. Dynamic measurements are carried out during these two tests, as well as measurements in statics, after the two shots, the object being to compare the state of the structure before and after application of the dynamic loading. The third test is an extreme load, with a large amount of explosive (163kg), located near the walls. The objectives of this last test are to characterize the peaks of effort before collapse as well as the type of collapse for each configuration. In this paper, only the results of the third test are presented. Position of the explosives is given in Figure 10.

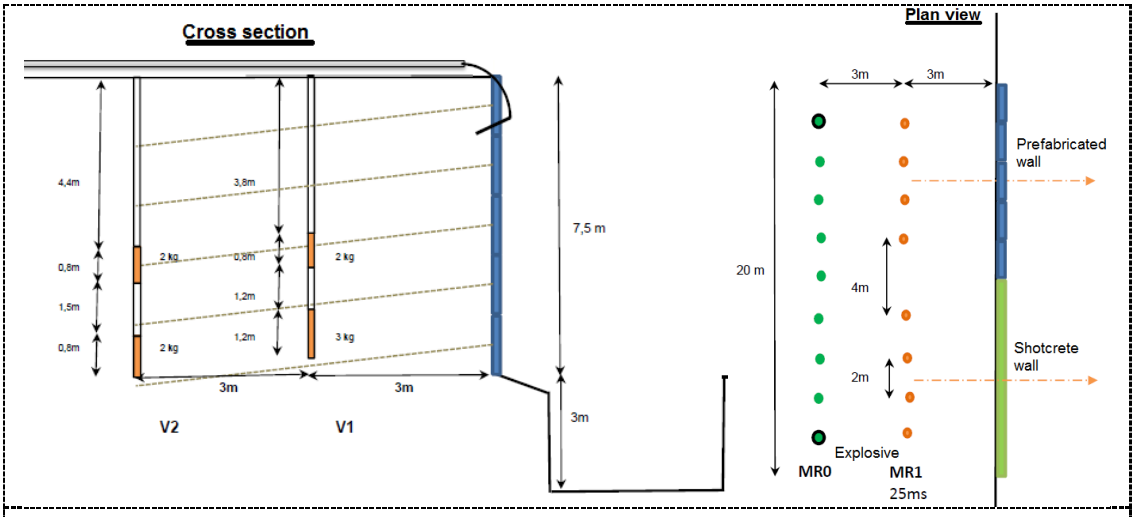

Figure 10. Position of the explosives

For the dynamic measurement associated with "ultimate" test (165kg of explosive), the initial zero of the various sensors was recalibrated, in order to clearly identify the maximum value of deformation induced in the nails (and therefore the force) induced by the shot of explosive undergone. It also allows us to easily compare behavior between different measurement points. We recall that the limit of the force sensor used is 20 tons, and that the gauges are glued at several points along the anchoring nails, in order to measure the distribution of deformation along the nail. From the deformation, we go back to the equivalent force. On each measuring point there are two gauges glued in opposition side. If the

measured strain is positive, the cable is in traction. If the measured strain is negative, the cable is compressive or flexural (thus with a gauge in compression and one in traction). In a measurement position, if a gauge gives a positive deformation, while the one opposite gives a negative deformation, then the nail works well in flexion, this is particularly the case at the neighborhood of the slab.
Note that the elastic limit of the nails (Ø25mm) of the wall is 670MPa, which corresponds to a maximum elastic deformation of 3190μm/m and a maximum equivalent force of 330kN. So, for a deformation higher than 3190μm/m, we can conclude to the plastic of the nail, and we do not have directly the value of the force. The acquisition frequency of the dynamic measurement is 10kHz (ten thousand points per second). Note that for dynamic testing, we found that some sensors did not work.

Important damage is observed at the base (foot) of the wall. (Figure 11) For the shotcrete wall, the mode of ruin is due to bending. This wall behaves like a continuous structure. Its behavior is similar to reinforced concrete voile subjected to dynamic out-of-plane loading (pressure). For the precast wall, the mode of ruin is also observed at the foot of the structure (two lines of low slabs). In particular, the failure mainly focuses on the 3 slabs in the center of each line, there are 5 slabs in total on each line, so 2 slabs at the edges ensure boundary conditions like two lateral supports. An important point to note while observing the collapse of the wall in slabs: the ruin is due to the rupture at the level of the joints (point of connection of the slabs) we do not see damage in the body of the slabs. These last ones undergo essentially rotations.

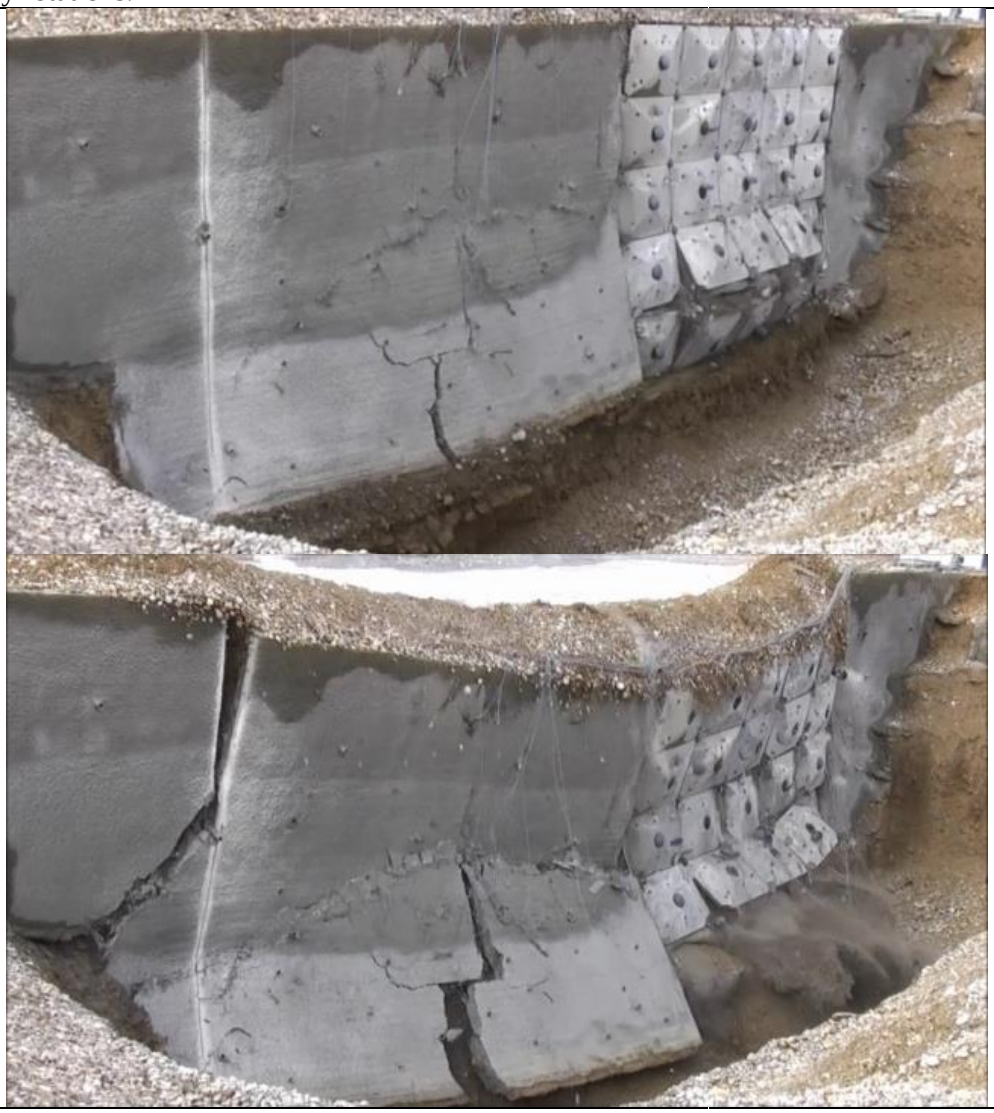

Figure 11. Collapse mode of two nail walls under explosion

Finally, it appears clearly on the film associated with the test, that the collapse first appears on the shotcrete wall, the collapse of the latter causes that of the precast wall. The latter because of the possible rotation of the slabs is more resistant and shows more resilience compared to the monolithic wall, in that it can develop a local "collapse" associated with large rotations on one or two slabs without the wall collapses.

For the precast wall, we note just before t = 0.24s the presence of peaks and oscillation that reflect the occurrence of the explosion (Figure 12). Beyond 5/100th of a second translate the behavior to collapse. There is indeed a flexion of the slab: the nail is subjected the compression (for a strain gauge) and for the other of the traction. The measured deformations remain however limited, although the rotation at the nail head of the slab is consequent.

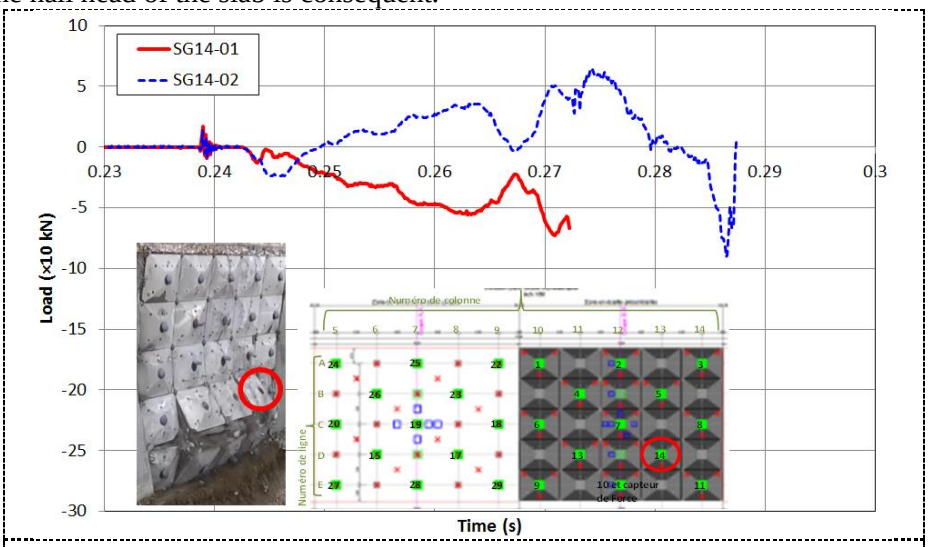

Figure 12. Load measured on the anchor nails of precast wall: SG14

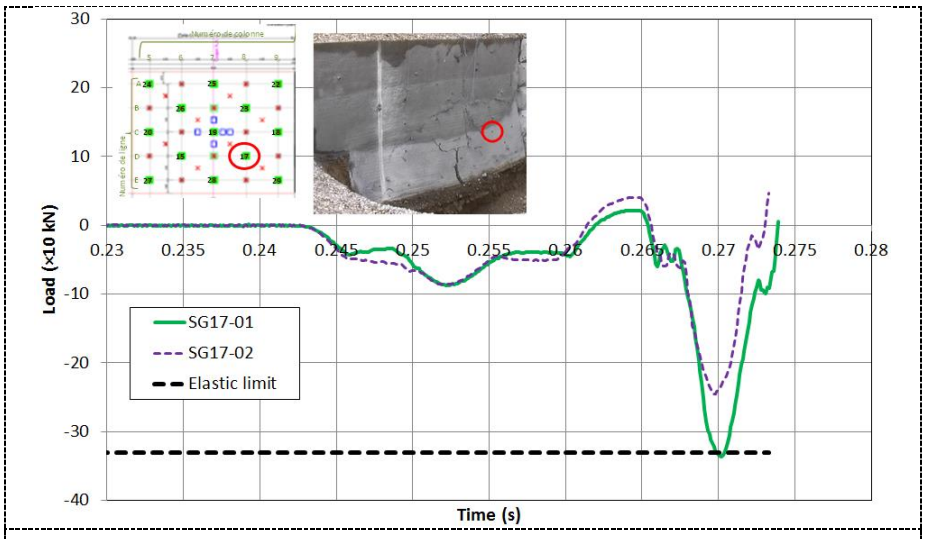

Figure 13. Load measured on the anchor nails of shotcrete wall: SG17

For the shotcrete wall (Figure 13), traction is obvious and this is the main mode of deformation (little bending), which is explained by the continuous and monolithic character of the wall. The latter undergoes essentially thrust and thus an "extension" out-of-plane, the local rotations are obtained ultimately to rupture and essentially to the right of the lines of rupture that do not pass through anchors. There are effort thresholds leading to the plastic of the anchor nail. The first compressive phase translates the propagation of the wave in the nail. It is transformed into traction once arrived at height of the wall.

5. Conclusion

This study presents the behaviour of a new concept of the soil nail wall using precast slabs. To gauge accurately the differences with classical shotcrete soil nail wall, a comparative in situ study was conducted including all the phases from the construction to the in-situ static measurements over two years and the in-situ dynamic tests under explosion demonstrated the robustness of the precast soil nail wall in comparing with the shotcrete wall. The laboratory testing on the precast slabs confirm the performance in mechanical properties of the constituent elements of the precast soil nail walls. The numerical model successfully reproduced the nonlinear behaviour of the experimental tests. Therefore this numerical model can be used in perspective to model the full wall constituted from the precast slabs elements. Furthermore, the use of precast slabs for the construction of nail walls provides solutions to many existing problems currently compared with shotcrete wall including:

- The delay: no phase reinforcement / formwork / drying
- Hygiene: no dust and noise when making the wall
- Safety: no risk related to concrete projection by air pressure
- Local environmental impact: no loss of concrete left in place
- The carbon footprint is divided by three by reducing the consumption of cement and use of eco-materials
- Geometric tolerances: the thicknesses of concrete are respected
- Weather dependence: no problem with this technique

References

[1] Chavan D, Mondal G and Prashant A 2017 Seismic analysis of nail soil slope considering interface effects *Soil Dyn Earthq Eng* vol 100 pp 480–490.
[2] Colin JG, Chouery-Curtis VE and Berg RR 1992 Field observations of reinforced soil structures under seismic loading *Proceedings of the international symposium on earth reinforcement* Fukuoka Japan vol 1 pp 223–228.
[3] Tatsuoka F, Tateyama M, Koseki J and Uchimura T 1995 Geotextile-reinforced soil retaining wall and their seismic behaviour *Proceedings of 10th Asian regional conferonce on soil mechanics and foundation engineering* vol 2 pp 26–49.
[4] Bui T T and Limam A 2015 Paroi clouée préfabriquée*:* Evaluation de la capacité portante d'une écaille constitutive: approche expérimentale et numérique *Internal report.*
[5] Bui T T and Limam A 2015 Parois clouées: Suivi du comportement sur chantier *Internal report.*
[6] Lee J and Fenves G 1998 Plastic-damage model for cyclic loading of concrete structures *Journal of Engineering Mechanics* vol 124 pp 892–900.
[7] Lubliner J, Oliver J, Oller S and Oñate E 1989 A plastic-damage model for concrete *International Journal of Solids and Structures* vol 25 pp 299–326.

Acknowledgments

This work was funded by contract from GTS Group NGE Lyon in France.